Composite Structures 105 (2013) 14–28

Contents lists available at SciVerse ScienceDirect

Composite Structures

journal homepage: www.elsevier.com/locate/compstruct

Dynamics of thin-walled composite beams: Analysis of parametric uncertainties

M.T. Piovan [a,*], J.M. Ramirez [a], R. Sampaio [b]

[a] Universidad Tecnológica Nacional – F.R.B.B., Centro de Investigaciones en Mecánica Teórica y Aplicada, 11 de Abril 461, Bahía Blanca, BA B8000LMI, Argentina
[b] PUC-Rio, Mechanical Engineering Department, Rua Marquês de São Vicente 225, Rio de Janeiro, RJ-22453-90 Rio de Janeiro, Brazil

ARTICLE INFO

Article history:
Available online 14 May 2013

Keywords:
Uncertainty quantification
Thin-walled beams
Dynamics
Composite materials
Parametric probabilistic approach
Shear deformability

ABSTRACT

This article is concerned with the stochastic dynamic analysis of structures constructed with composite materials. Depending on many aspects (manufacturing process, material uncertainty, boundary conditions, etc.) real composite structures may have deviations with respect to the calculated response (or deterministic response). These aspects lead to a source of uncertainty in the structural response associated with constituent proportions, geometric parameters or other unexpected agents. Uncertainties should be considered in a structural system in order to improve the predictability of a given modeling scheme. In this study a model of shear deformable composite beams is employed as the mean model. The probabilistic model is constructed by adopting random variables for the uncertain parameters of the model. This strategy is called parametric probabilistic approach. The probability density functions of the random variables are constructed appealing to the Maximum Entropy Principle. The continuous model is discretised by finite elements and the Monte Carlo method is employed to perform the simulations, thereafter a statistical analysis is performed. Numerical studies are carried out to show the main advantages of the modeling strategies employed, as well as to quantify the propagation of the uncertainty in the dynamics of slender composite structures.

1. Introduction

Composite materials have many advantages with respect to isotropic materials that motivate their use as structural components. The most well known properties of composite materials are high strength and stiffness properties together with a low weight, good corrosion resistance, enhanced fatigue life, low thermal expansion properties, among others [1]. Other important feature of composite materials is the very low machining cost for complex structures [2,3]. As a result of the increasing use of thin-walled composite beams, the analysis of static and dynamic behavior is a task of intense research. Since the eighties many research activities are being devoted toward the development of theoretical and computational methods for the appropriate analysis of such members. The first consistent study dealing with the static structural behavior of thin-walled composite-orthotropic members, under various loading patterns, was due to Bauld and Tseng [4], who developed in the early eighties, invoking Vlasov hypotheses, a beam theory to analyze fiber-reinforced members featuring open cross-sections with symmetric laminates. This theory assumed the cross-sections to be shear undeformable and was restricted to members formed by non-general stacking sequences and employed only for static analysis. Further contributions of many authors [5] until the present time, made possible the extension of Vlasov models by considering shear deformability due to bending and warping effects, among others, and the resulting models were employed in many problems.

Thin-walled composite beam-models allowing for some effects of shear deformability were presented, in the middle eighties in the work of Bauchau [6]. In this article, the effect of full shear deformability, specially the warping torsion shear deformability, was not taken into account or was slightly studied in a few problems of statics and dynamics. The late eighties and the nineties brought a considerable amount of new models and uses. Rehfield and Atilgan [7] studied the non-conventional effects of constitutive elastic couplings (such as bending–bending coupling or bending-shear coupling) in the mechanics of cantilever box-beams. In the models developed by Librescu and Song [8] and Song and Librescu [9], that were largely applied as a basis of a broad research on composite beams, the bending component of shear flexibility was considered but the shear deformation due to warping torsion component was neglected. However in these models new extensions were performed, such as the accounting for the effect of the shell-thickness in shear and warping deformations. Special attention deserve the works of Cesnik et al. [10], who performed

* Corresponding author. Tel.: +54 291 4555220; fax: +54 291 4555311.
E-mail address: mpiovan@frbb.utn.edu.ar (M.T. Piovan).

0263-8223/$ - see front matter © 2013 Elsevier Ltd. All rights reserved.
http://dx.doi.org/10.1016/j.compstruct.2013.04.039

studies on thin-walled composite beams by means of the so-called Variational Asymptotical Cross Sectional Analysis (VABSA) Method. In these works there is no mention to buckling problems and vibrations with states of arbitrary initial stresses. Employing the Hellinger–Reissner principle, Cortínez and Piovan [11] introduced a theory of thin-walled beams with symmetric balanced laminates, which considers full shear flexibility, i.e. bending shear deformation and torsion-warping shear deformation. This model covers topics of dynamics under states of initial normal stresses, and also accounts for thickness shear flexibility and warping. Many of the aforementioned models were employed only for static response or for eigenvalue calculation. Piovan and Cortínez [12,13] extended the previous model by incorporating general laminates, buckling analysis and other complexities such as beams with curved axis among others. Especial attention deserves a group of new interesting models for composite beams that have been developed recently appealing to unified formulations and enriched kinematics [14–16,18,17]. Particularly, the works of Carrera and Varelo [16] and Giunta et al. [15] are devoted to thin-walled composite beams accounting for shear flexibility as well as other types of non-conventional effects. This type of modeling incorporates an enriched kinematics that consists in the common degrees of freedom of a beam (centroid displacements and rotations) and higher order terms associated to non-conventional degrees of freedom. The shear flexible models of Piovan and Cortínez [12,13], although with a simpler kinematics than the previous ones, can also reach a quite good correspondence with respect to the available experimental data for the mechanics of beams through the appropriate involvement of the few most relevant kinematic variables [12,29]. This is a crucial aspect for problems with highly demanding computational cost such as the structural optimization or the quantification of uncertainty in dynamics of composite beams, among others.

The uncertainty is an important concern in the behavior of beams constructed with fiber reinforced composite materials due to their inherent variability. The first studies about the quantification of uncertainty in composite materials are related to the constituent level, fibre/matrix or ply level according to the deep review of the state of the art carried out by Sriramula and Chryssantopoulos [19]. The main sources of uncertainty in composite materials are the value of constituent properties at microscopic level, geometric aspects at mesoscale or macroscopic level and the manufacturing and machining processes. The manufacturing processes of composite structures may affect strongly the dynamic response. There is a huge amount of research related to quantifying the propagation of uncertainty in the mechanics of composite materials at the microscale/macroscale levels [19] or in the quite sensitive case of failure analysis [20,33] or in dynamics of composite plates [21], among others.

There are different approaches to evaluate the dynamic response of structures subjected to several aspects of uncertainty. The most common is the consideration of the uncertainty in loads, or external excitations, as a random processes [22]. The uncertainty involved in the material properties of the composites can be considered as random fields according to the works of Onkar et al. [23] and Mehrez et al. [24,25] among others. Other way to study the dynamic response due to uncertainties in the composite material is associating random variables to given parameters that are considered uncertain, which is called parametric probabilistic approach [26]. The construction or derivation of the probability density functions of the random variables is a crucial task that needs some information about the statistics of the parameters (e.g. expected value or bounds and/or coefficient of variation). The Maximum Entropy Principle [27] is employed to construct the stochastic model of the structure. Within this context, the probability density functions of random variables are deduced in order to guarantee that they achieve the maximum uncertainty which is measured in terms of entropy defined according to Shannon [28]. This is the approach to be employed in the present article. The basic elastic properties of a layer and orientation angles of the laminates are assumed to vary around the expected values (that shape the deterministic model), then two sets of random variables (one for material properties and other for orientation angles) are introduced and their corresponding probability density function are adopted with the aid of the Maximum Entropy Principle. The deterministic and probabilistic approaches of the structural model are formulated in a continuous and discretised by the finite element method. The Monte Carlo Method is used to obtain the statistics of the dynamic response associated to a number of independent simulations.

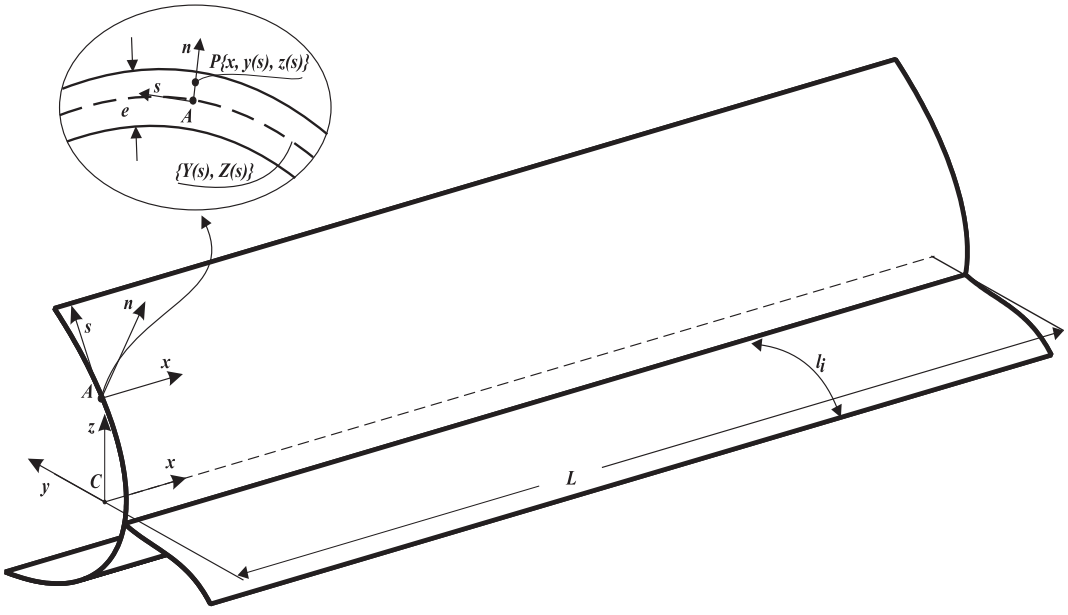

Fig. 1. Thin-walled beam with reference systems.

The article is organized as follows: after the introductory section where the state-of-the-art is summarized, the deterministic continuous model and its finite element discretisation are briefly described, then the probabilistic model is constructed. The subsequent sections contain the computational studies: a validation of the deterministic beam model with 3D finite element approaches and the analysis of the uncertainty propagation in the dynamics of thin-walled composite beams and, finally, concluding remarks are outlined.

2. Model development

2.1. Brief representation of the composite beam model

In Fig. 1 a basic sketch of the thin-walled beam is shown, where it is possible to see the reference systems {**C**:*xyz*} and {**A**:*xsn*}. The principal reference point **C** is located at the geometric center of the cross-section, where the *x*-axis is parallel to the longitudinal axis of the beam while *y* and *z* are the axes of the cross section, but not necessarily the principal axes of inertias. The secondary reference system {**A**:*xsn*}, is used to describe shell stresses and strains as common practice for thin-walled composite beams [1]. The point **A** is located in the mid surface of the wall, whereas *s*-axis and *n*-axis are respectively tangent and normal to the mid surface, as it is possible to see in the detail of Fig. 1, where *e* is the thickness of the wall. Depending on the features of the cross-section it is useful to define more than one secondary system as shown in Fig. 2. The thin-walled beam model is based in the following assumptions [11,12]:

(1) The cross-section contour is rigid in its own plane.
(2) The radius of curvature at any point of the shell is neglected. This implies to consider the section shaped in a polygonal arrangement.
(3) The warping function is normalized with respect to the principal reference point **C**.
(4) A general laminate stacking sequence for composite material is considered.
(5) The material density is considered constant along the beam axis but it can vary in the laminate thickness.
(6) The stress components σ_{xx}, σ_{xs} and σ_{xn} and the strains and curvature components ϵ_{xx}, γ_{xs}, γ_{xn}, κ_{xx} and κ_{xs} are the most representative, whereas remaining components are assumed negligible.
(7) The model is described in the context of linear elasticity.

2.2. Governing equations and boundary conditions

Following Assumptions (1)–(7) it is possible to derive the displacement field of an arbitrary point **P** [12,29] of the beam, which can be presented in the subsequent form:

$$\widetilde{\mathbf{U}}_{\boldsymbol{P}} = \begin{Bmatrix} u_x \\ u_y \\ u_z \end{Bmatrix} = \begin{Bmatrix} u_{xc} - \omega\theta_x \\ u_{yc} \\ u_{zc} \end{Bmatrix} + \begin{bmatrix} 0 & -\theta_z & \theta_y \\ \theta_z & 0 & -\phi_x \\ -\theta_y & \phi_x & 0 \end{bmatrix} \begin{Bmatrix} 0 \\ y \\ z \end{Bmatrix}, \tag{1}$$

where u_{xc}, u_{yc}, u_{zc} are the displacements of the reference center in *x*-, *y*-, and *z*-directions, respectively. θ_z and θ_y are bending rotational parameters. ϕ_x is the twisting angle and θ_x is a warping-intensity parameter. The cross-sectional coordinates of the reference system {**C**:*xyz*} can be expressed in terms of the cross-sectional coordinates of the reference system {**A**:*xsn*} and the coordinates of the middle line of the wall [29,37,38]. Thus, in Eq. (1) the cross-sectional coordinates $y(s)$ and $z(s)$ of a generic point **P** are related to the ones of the wall middle line $Y(s)$ and $Z(s)$ by means of Eq. (2). The warping function normalized with respect to the reference system {**C**:*xyz*} is defined in Eq. (3).

$$y(s) = Y(s) - n\frac{dZ}{ds}, \quad z(s) = Z(s) + n\frac{dY}{ds}, \tag{2}$$

$$\omega(s,n) = \omega_p(s) + \omega_s(s,n). \tag{3}$$

In Eq. (3), $\omega_p(s)$ is the primary or contour warping function, whereas $\omega_s(s,n)$ is the secondary, or thickness, warping. These entities are given by:

$$\omega_p(s) = \int_0^s [r(s) + \psi(s)]ds - D_C, \quad \omega_s(s,n) = -nl(s), \tag{4}$$

where the functions $r(s)$, $l(s)$, $\psi(s)$ and D_C are defined in the following form:

$$r(s) = Z(s)\frac{dY}{ds} - Y(s)\frac{dZ}{ds}, \quad l(s) = Y(s)\frac{dY}{ds} + Z(s)\frac{dZ}{ds},$$
$$\psi(s) = \frac{1}{\overline{A}_{66}(s)}\left[\frac{\int_0^s r(s)ds}{\oint_S \frac{1}{\overline{A}_{66}(s)}ds}\right], \quad D_C = \frac{\oint_S [r(s) + \psi(s)]\overline{A}_{11}(s)ds}{\oint_S \overline{A}_{11}(s)ds}. \tag{5}$$

The functions $\overline{A}_{11}$ and $\overline{A}_{66}$ are normal and tangential elastic properties of composite laminates [11] which can vary along the cross-sectional middle line. The function $\psi(s)$ is connected with

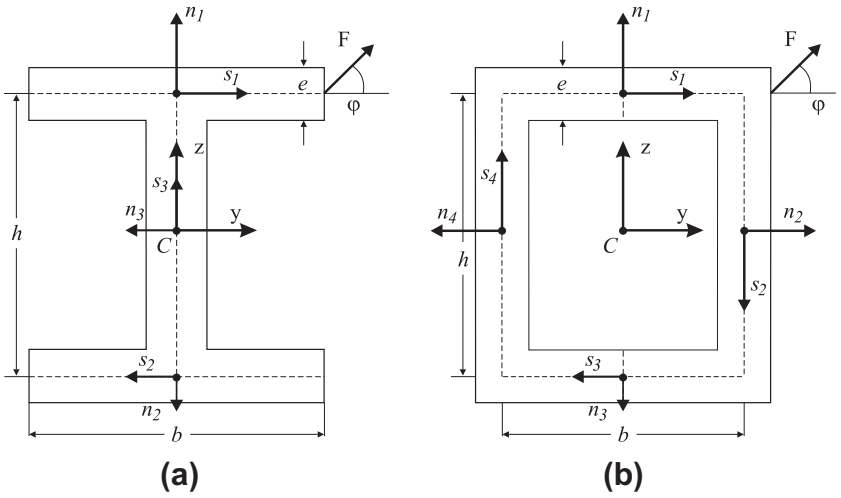

Fig. 2. Features of cross-section profiles (a) open and (b) closed.

the torsional shear flow and D_C is a constant for normalization of the warping function with respect to the reference system {***C***:*xyz*} [11,29]. $\mathcal{S}$ is the domain of the cross-sectional middle line. In the case of open sections the function $\psi(s) = 0$, consequently Eq. (4) holds for both closed and open sections. The warping function described in Eq. (3), has an analogous form to the ones defined by Song and Librescu [9] or Na and Librescu [30] for closed sections.

The displacement–strain relations can be obtained by substituting Eq. (1) in the well-known expressions of linear strain components. As it was shown by Piovan [29] or Piovan and Cortínez [12] the shell strains can be written as:

$$\widetilde{\mathbf{E}}_P = \mathbf{G}_k \widetilde{\mathbf{D}}, \tag{6}$$

where

$$\begin{aligned} \widetilde{\mathbf{E}}_P^T &= \{\epsilon_{xx}, \gamma_{xs}, \gamma_{xn}, \kappa_{xx}, \kappa_{xs}\}, \\ \widetilde{\mathbf{D}}^T &= \{\varepsilon_{D1}, \varepsilon_{D2}, \varepsilon_{D3}, \varepsilon_{D4}, \varepsilon_{D5}, \varepsilon_{D6}, \varepsilon_{D7}, \varepsilon_{D8}\}, \end{aligned} \tag{7}$$

$$\mathbf{G}_k = \begin{bmatrix} 1 & Z & -Y & -\omega_p & 0 & 0 & 0 & 0 \\ 0 & 0 & 0 & 0 & dY/ds & dZ/ds & r(s)+\psi(s) & -\psi(s) \\ 0 & 0 & 0 & 0 & -dZ/ds & dY/ds & l(s) & 0 \\ 0 & -dY/ds & dZ/ds & -l(s) & 0 & 0 & 0 & 0 \\ 0 & 0 & 0 & 0 & 0 & 0 & 1 & -2 \end{bmatrix}. \tag{8}$$

In Eq. (7), ϵ_{xx}, γ_{xs} and γ_{xn} are the strain components and κ_{xx}, κ_{xs} are the curvatures of the shell that conforms the wall of the cross-section. These strain components are measured according to the wall reference system {***A***:*xsn*}. The entities ε_{Di}, $i = 1, \ldots, 8$ may be regarded as generalized deformations. In this context ε_{D1} is the axial deformation, ε_{D2} and ε_{D3} are bending deformations, ε_{D4} is the deformation due to non-uniform warping, ε_{D5} and ε_{D6} are the bending shear deformations, ε_{D7} is the warping shear deformation and finally ε_{D8} is the pure torsion shear deformation. These generalized deformations, which are collected in vector $\widetilde{\mathbf{D}}$, are defined in the following form:

$$\widetilde{\mathbf{D}} = \mathbf{G}_{DU} \widetilde{\mathbf{U}}, \tag{9}$$

where $\mathbf{G}_{DU}$ is a matrix operator and $\widetilde{\mathbf{U}}$ is the vector of kinematic variables which are defined in following forms, in which $\partial_x(\diamondsuit)$ is the spatial derivative operator.

$$\mathbf{G}_{DU} = \begin{bmatrix} \partial_x(\diamondsuit) & 0 & 0 & 0 & 0 & 0 & 0 \\ 0 & 0 & 0 & 0 & \partial_x(\diamondsuit) & 0 & 0 \\ 0 & 0 & \partial_x(\diamondsuit) & 0 & 0 & 0 & 0 \\ 0 & 0 & 0 & 0 & 0 & 0 & \partial_x(\diamondsuit) \\ 0 & \partial_x(\diamondsuit) & -1 & 0 & 0 & 0 & 0 \\ 0 & 0 & 0 & \partial_x(\diamondsuit) & 1 & 0 & 0 \\ 0 & 0 & 0 & 0 & 0 & \partial_x(\diamondsuit) & -1 \\ 0 & 0 & 0 & 0 & 0 & \partial_x(\diamondsuit) & 0 \end{bmatrix}, \tag{10}$$

$$\widetilde{\mathbf{U}}^T = \{u_{xc}, u_{yc}, \theta_z, u_{zc}, \theta_y, \phi_x, \theta_x\}. \tag{11}$$

The principle of virtual works can be condensed in the following form:

$$\begin{aligned} \mathcal{W}_T = &\int_L (\delta \widetilde{\mathbf{D}}^T \widetilde{\mathbf{Q}}) dx + \int_L \delta \widetilde{\mathbf{U}}^T \mathbf{M}_m \ddot{\widetilde{\mathbf{U}}} \, dx - \int_L \delta \widetilde{\mathbf{U}}^T \widetilde{\mathbf{P}}_X \, dx \\ &+ \delta \widetilde{\mathbf{U}}^T \widetilde{\mathbf{B}}_X \big|_{x=0}^{x=L} \\ = &\, 0, \end{aligned} \tag{12}$$

where the force vector $\widetilde{\mathbf{Q}}$ is defined as follows:

$$\widetilde{\mathbf{Q}}^T = \{Q_x, M_y, M_z, B, Q_y, Q_z, T_w, T_{sv}\}, \tag{13}$$

whereas for the sake of smooth reading, the matrix of mass coefficients $\mathbf{M}_m$, the vector of external forces $\widetilde{\mathbf{P}}_X$, and the vector of natural boundaries conditions $\widetilde{\mathbf{B}}_X$ are detailed in Appendix A.

In Eq. (13) the internal beam forces Q_x, M_y, M_z, and B correspond to the axial force, the bending moment in *y*-direction, the bending moment in *z*-direction, and the bi-moment, respectively; whereas the internal forces Q_y, Q_z, T_w, and T_{sv} correspond to the shear force in *y*-direction, the shear force in *z*-direction, the twisting moment due to warping and the twisting moment due to pure torsion, respectively. These internal forces can be written in terms of the shell-forces as [12]:

$$\widetilde{\mathbf{Q}} = \int_{\mathcal{S}} \mathbf{G}_k^T \widetilde{\mathbf{N}}_P \, ds, \tag{14}$$

where $\widetilde{\mathbf{N}}_P$ is the vector of shell stress resultants or shell forces and moments defined according to [1–3]:

$$\widetilde{\mathbf{N}}_P^T = \int_{-e/2}^{e/2} \{\sigma_{xx}, \sigma_{xs}, \sigma_{xn}, n\sigma_{xx}, n\sigma_{xs}\} dn. \tag{15}$$

The differential equations of motion and associated boundary conditions can be derived by applying the conventional steps of variational calculus to Eq. (12). The differential equations of motion can be useful for some numerical methods, e.g. power series method. While in the present article the finite element method is employed, the derivation of differential equations is not necessary. The interested reader may follow, in the works of Piovan and Cortínez [12] and Piovan [29], the form and features of the differential equations of the thin-walled composite beam models applied to several problems of mechanics of beams.

2.3. Constitutive equations

In order to obtain the relationship between generalized beam forces (or beam stress resultants) and generalized deformations ε_{Di}, one has to select the constitutive laws for a composite shell [1,3] and employ appropriate constitutive hypotheses [12] of the shell stress resultants in terms of the shell strains. The shell stress resultants can be expressed in terms of the generalized deformations defined in Eq. (9) in the following matrix form:

$$\widetilde{\mathbf{N}}_P = \mathbf{M}_C \widetilde{\mathbf{E}}_P, \tag{16}$$

where $\mathbf{M}_C$ is the matrix of modified shell stiffness, which depends on the type of constitutive hypotheses involved [12,29] and can be expressed in the following form:

$$\mathbf{M}_C = \begin{bmatrix} \overline{A}_{11} & \overline{A}_{16} & 0 & \overline{B}_{11} & \overline{B}_{16} \\ & \overline{A}_{66} & 0 & \overline{B}_{16}^* & \overline{B}_{66} \\ & & \overline{A}_{55}^* & 0 & 0 \\ & sym & & \overline{D}_{11} & \overline{D}_{16} \\ & & & & \overline{D}_{66} \end{bmatrix}. \tag{17}$$

Due to the lack of space the coefficients $\overline{A}_{11}$, $\overline{B}_{11}$, $\overline{D}_{11}$, etc., are not described in the present article, however the reader can find them in the works of Piovan and Cortínez [12].

Substituting Eq. (16) into Eq. (14) the beam stress resultants can be obtained in terms of generalized strains:

$$\widetilde{\mathbf{Q}} = \mathbf{M}_k \widetilde{\mathbf{D}}, \tag{18}$$

where

$$\mathbf{M}_k = \int_{\mathcal{S}} \mathbf{G}_k^T \mathbf{M}_C \mathbf{G}_k \, ds. \tag{19}$$

The matrix $\mathbf{M}_k$ of cross-sectional stiffness coefficients, leads to constitutive elastic coupling or not, depending on the stacking sequence of the laminates in a given cross-section. That is, for example, if the laminates are specially orthotropic or cross-ply, or specially symmetric balanced, there is no constitutive elastic coupling [11], however if the laminates are general the beam could have different types of constitutive elastic couplings such as twisting-bending-extensional coupling, extensional-bending coupling and bending–bending coupling [7,12,29,38].

2.4. Finite element approach

In order to solve problems of dynamics with several boundary conditions, quartic order isoparametric finite elements are employed. These elements have five nodes and seven degrees-of-freedom per node [12], that is the kinematic variables of Eq. (11).

Applying the conventional discretiztion techniques and variational procedures [31] in Eq. (12), the following finite element equation is attained:

$$\mathbf{K}\overline{\mathbf{W}} + \mathbf{M}\ddot{\overline{\mathbf{W}}} = \overline{\mathbf{F}}, \tag{20}$$

where $\mathbf{K}$ and $\mathbf{M}$ are the global matrices of elastic stiffness and mass, respectively; whereas $\overline{\mathbf{W}}$, $\ddot{\overline{\mathbf{W}}}$ and $\overline{\mathbf{F}}$ are the global vectors of nodal displacements, nodal accelerations and nodal forces, respectively.

Eq. (20) can be modified in order to account for "a posteriori" structural proportional Rayleigh damping given by:

$$\mathbf{C}_{RD} = \eta_1\mathbf{M} + \eta_2\mathbf{K}. \tag{21}$$

The coefficients η_1 and η_2 in Eq. (21) can be computed using two given damping coefficients (namely, ξ_1 and ξ_2) for the first and second modes, according to the common methodology presented in the bibliography related to finite element procedures [31,32]. The matrices $\mathbf{M}$ and $\mathbf{K}$ are the global mass matrix and the global elastic stiffness matrix, respectively. This leads to:

$$\mathbf{K}\overline{\mathbf{W}} + \mathbf{C}_{RD}\dot{\overline{\mathbf{W}}} + \mathbf{M}\ddot{\overline{\mathbf{W}}} = \overline{\mathbf{F}}. \tag{22}$$

The response in the frequency domain of the linear dynamic system given by Eq. (22) can be written as [32]:

$$\widehat{\mathbf{W}}(\omega) = [-\omega^2\mathbf{M} + i\omega\mathbf{C}_{RD} + \mathbf{K}]^{-1}\widehat{\mathbf{F}}(\omega), \tag{23}$$

where $\widehat{\mathbf{W}}$ and $\widehat{\mathbf{F}}$ are the Fourier transform of the displacement vector and force vector, respectively; whereas ω is the circular frequency measured in [rad/s].

3. Stochastic model

The Maximum Entropy Principle [27] is employed to construct the stochastic model with the uncertain parameters. The stochastic model is constructed selecting two sets of uncertain parameters and associating random variables to them. One set for the orientation angles of the fiber reinforcement in the layers of each panel and other set for basic elastic properties of the material. The construction of the probability density functions of the random variables is quite sensitive in stochastic analysis and they should be deduced according to the given information (frequently scarce) about the uncertain parameters. The Maximum Entropy Principle offers a consistent strategy, in the authors' opinion, to select the probabilistic model despite the lack of experimental data. Thus, the Maximum Entropy Principle allows to derive the probability density functions of the random variables guaranteeing consistence with the available information and the physics of the problem. In the present problem random variables V_i, $i = 1, 2, \ldots, N_P$ and V_i, $i = N_P + 1, \ldots, N_P + 6$ are introduced such that they represent the angles of N_P different plies in a cross-sectional laminate and the basic elastic properties of the material (i.e. elastic moduli: E_{11}, $E_{22} = E_{33}$, $G_{12} = G_{13}$ and G_{23}, Poisson coefficients: $\nu_{12} = \nu_{13}$ and ν_{23}), respectively.

The probability density functions of the random variables can be obtained by means of the following optimization problem:

$$p_V^{(opt)} = \arg\max_{p_V \in \mathfrak{P}} S(p_V), \tag{24}$$

where $p_V^{(opt)}$ is the optimal probability density function such that $S\left(p_V^{(opt)}\right) \geqslant S(p_V),\ \forall p_V \in \mathfrak{P}$, and S is the entropy measure, whereas $\mathfrak{P}$ is the set of admissible probability density functions satisfying the known data of the random variables and the physical constraints. The measure of the entropy is defined as [28]:

$$S(p_V) = -\int_{\mathfrak{S}} p_V \ln(p_V) dv \tag{25}$$

where $\mathfrak{S}$ is the support of the probability distributions of the random variables taken into account in the optimization procedure.

The available information to obtain the probability density functions of both sets of random variables is related to some information extracted from the technical literature, the expected mistakes in the construction process and some assumptions. Thus, the nominal values of the parameters in the deterministic model are assumed to be the mean of the random variables, consequently the expected values are $\mathcal{E}\{V_i\} = \underline{V}_i$, $i = 1, \ldots, N_P + 6$. The random variables V_i, $i = 1, \ldots, N_P$ have bounded supports whose upper and lower limits are distant Δ_α from the expected value $\underline{V}_i$. Moreover, the construction of the laminates should maintain the condition of symmetry (anti-symmetry) in the corresponding cases. Random variables V_i, $i = N_P + 1, \ldots, N_P + 6$ should be strictly positive and should have bounded supports. According to the compilation report carried out by Sriramula and Chryssanthopoulos [19] there is evidence that the support function of elastic properties for carbon/epoxy and graphite/epoxy prepegs fall within the bounds defined by a coefficient of variation $\delta_{V_i} \in [0.04, 0.12]$, $i = N_P + 1, \ldots, N_P + 6$. The expected value and the coefficient of variation are necessary to calculate the variance of the random variable, $\mathrm{var}(V_i) = (\underline{V}_i\delta_{V_i})^2$, $i = N_P + 1, \ldots, N_P + 6$, that has to be kept finite in order to guarantee the physical consistency of the problem. If there is no information about the relation or dependency among random variables, the Maximum Entropy Principle states that the random variables must be independent. Moreover if the random variable is bounded, the Maximum Entropy Principle states that the probability distribution is uniform.

At this point, a few remarks have to be mentioned. As it was indicated by Sriramula and Chryssanthopoulos [19], many reports of the technical literature ([34,35] among others) simulated 'empirical' random variable models on the basis of certain experimental evidence and engineering judgement. However probability laws such as Normal, Weibull, Gamma or Log Normal distributions (which are unbounded or bounded on the left) were used in those papers. Since basic elastic properties must characterize a real material in service, the occurrence of cases of the random variable tending to zero or infinity and outside given limits are meaningless and not consistent with the reality of the material.

Consequently, according to the aforementioned background, the probability density functions of the random variables V_i can be written as:

$$p_{V_i}(v_i) = \mathfrak{S}_{[\mathcal{L}_{V_i}\,\mathcal{U}_{V_i}]}(v_i)\frac{1}{2\Delta_\alpha}, \quad i = 1, \ldots, N_P \tag{26}$$

$$p_{V_i}(v_i) = \mathfrak{S}_{[\mathcal{L}_{V_i}\,\mathcal{U}_{V_i}]}(v_i)\frac{1}{2\sqrt{3}\underline{V}_i\delta_{V_i}}, \quad i = N_P + 1, \ldots, N_P + 6 \tag{27}$$

where $\mathfrak{S}_{[\mathcal{L}_{V_i}\,\mathcal{U}_{V_i}]}(v_i)$ is the generic support function, whereas $\mathcal{L}_{V_i}$ and $\mathcal{U}_{V_i}$ are the lower and upper bounds of the random variable V_i. Δ_α is a gap measured in angular units (radians or degrees), whereas δ_{V_i} is the coefficient of variation. The Matlab function unifrnd ($\underline{V}_i - \Delta_\alpha$,

$\underline{V}_i + \Delta_\alpha$) can be used to generate realizations of the random variables V_i, $i = 1, 2, \ldots, N_P$. The Matlab function unifrnd $\left(\underline{V}_i\left(1-\delta_{V_i}\sqrt{3}\right), \underline{V}_i\left(1+\delta_{V_i}\sqrt{3}\right)\right)$ can be used to generate realizations of the random variables V_i, $i = N_P + 1, \ldots, N_P + 6$.

Then, using Eqs. (26) and (27) in the construction of the matrices of finite element model given in Eq. (23) the stochastic finite element model can be written as:

$$\widehat{\mathbb{W}}(\omega) = [-\omega^2\mathbf{M} + i\omega\mathbb{C}_{RD} + \mathbb{K}]^{-1}\widehat{\mathbf{F}}(\omega). \tag{28}$$

Notice that in Eq. (28) the math-blackboard typeface is employed to indicate stochastic entities, thus $\mathbb{K}$ is stochastic because Eq. (26) in employed in its derivation, and $\mathbb{C}_{RD}$ is stochastic through the stochastic nature of $\mathbb{K}$ in Eq. (21), hence $\widehat{\mathbb{W}}$ is stochastic.

The Monte Carlo method is used to simulate the stochastic dynamics, which implies the calculation of a deterministic system for each realization of random variables $\underline{V}_i$, $i = 1, 2, \ldots, N_P + 6$. The convergence of the stochastic response $\widehat{\mathbb{W}}$ is calculated appealing to the following function:

$$conv(N_{MS}) = \sqrt{\frac{1}{N_{MS}}\sum_{j=1}^{N_{MS}}\int_\Omega \|\widehat{\mathbb{W}}_j(\omega) - \widehat{\mathbf{W}}(\omega)\|^2 d\omega}, \tag{29}$$

where N_{MS} is the number of Monte Carlo samplings and Ω is the frequency band of analysis, whereas $\widehat{\mathbb{W}}$ is the response of the stochastic model and $\widehat{\mathbf{W}}$ the response of the mean model or deterministic model.

4. Computational studies

4.1. Validation of the deterministic beam model

In this section a validation of the deterministic beam model with higher finite element approaches is performed. Then the natural frequencies of the beam model are contrasted with the corresponding results of the commercial programs Abaqus (with 3D anisotropic finite elements). The beam has a closed cross-section with the following dimensions: height $h = 23.438$ mm, width $b = 12.838$ mm, thickness $e = 0.762$ mm as in Fig. 2. The material properties are: $E_{11} = 134.44$ GPa, $E_{22} = E_{33} = 18.00$ GPa, $G_{12} = G_{13} = 3.60$ GPa, $G_{23} = 5.00$ GPa, $\nu_{12} = \nu_{13} = 0.26$, $\nu_{23} = 0.30$, and the density $\rho = 1400$ kg/m^3. The cross-sectional panels have the same lamination scheme and three typical stacking sequences were selected for this study, namely $\{(0/90)\}_4$, $\{(0/30)\}_4$ and $\{0/0\}_4$. The beam is clamped (i.e. all kinematic variables are blocked) in one end and free in the other. Moreover, models of about 3200 solid 3D elements were prepared in Abaqus (actually C3D8R elements with linear interpolation and reduced integration, involving more than 52,000 degrees-of-freedom) in contrast of the 12 elements (that is, no more than 350 degrees-of-freedom) used to calculate the response of the beam model.

The first four natural frequencies calculated with one-dimensional, 1D, and three-dimensional, 3D, approaches are shown in Table 1. Furthermore in this table the vibratory character of each frequency is classified by means of the acronyms *BYY*, *BZZ*, *T* or *BYZ*; that is bending mode in *y*-direction, bending mode in *z*-direction and twisting mode or coupled bending–bending mode respectively. The use of these acronyms is intended for identifying the main feature (bending, twisting or coupled behavior) of the modes of a given beam structure. However the difference among the same class of acronym (e.g. *BYY*) employed in a given case is associated with different number of half-waves along the beam axis. A good correlation can be appreciated between both approaches and the percentage differences of 1D results with respect to the 3D ones are no greater than 9%. The interested reader can follow authors' references [29,12] for finding more validations and comparisons of the beam theory employed in the present paper.

Table 1
Comparison of the first four free vibration frequencies (Hz) of the composite beam model with the corresponding 3D finite element approach.

Laminate	h/L	Approach	f_1	f_2	f_3	f_4
$\{(0/90)_4\}$	0.0307	3D (Abaqus)	40.01	64.61	239.35	379.17
		1D (Present)	39.53	62.27	237.27	368.06
		Mode	*BZZ*	*BYY*	*BZZ*	*BYY*
	0.1	3D (Abaqus)	390.47	617.54	1389.50	1763.40
		1D (Present)	390.45	600.85	1368.63	1812.30
		Mode	*BZZ*	*BYY*	*T*	*BZZ*
$\{(0/30)_4\}$	0.0307	3D (Abaqus)	40.60	65.69	244.00	403.01
		1D (Present)	40.94	65.99	253.43	405.10
		Mode	*BZZ*	*BYZ*	*BZZ*	*BYZ*
	0.1	3D (Abaqus)	420.70	678.90	2077.90	2227.10
		1D (Present)	423.08	673.88	2267.07	2465.26
		Mode	*BZY*	*BYZ*	*BZY*	*T*
$\{(0/0)_4\}$	0.0307	3D (Abaqus)	51.82	82.91	298.26	425.09
		1D (Present)	52.31	82.02	304.82	418.73
		Mode	*BZZ*	*BYY*	*BZZ*	*T*
	0.1	3D (Abaqus)	481.09	747.33	1351.20	1921.00
		1D (Present)	493.78	747.39	1372.59	2051.12
		Mode	*BZZ*	*BYY*	*T*	*BZZ*

4.2. Uncertainty propagation in the dynamic response of thin-walled composite beams

In this section a study is carried out related to the propagation of uncertainties, due to material properties and/or constructive aspects of composite laminates, in the dynamic response of thin-walled composite beams. For this study a clamped-free thin-walled beam (length $L = 6.0$ m) with the cross-sections as sketched in Fig. 2 is employed. Note that Fig. 2 has a local reference system for each cross-sectional segment in order to simplify the stacking sequence description. Also in Fig. 2 one can see the excitation due to an impulsive unitary force located at $x, y, z = L, b/2, h/2$ and oriented with $\psi = 45°$. The web height and flange width are $h = 0.6$ m, $b = 0.3$ m, whereas the thickness of all laminates is $e = 0.03$ m. Each laminate is composed by eight laminas of equal thickness. The material of the beams is graphite–epoxy (AS4/3501-6) whose properties are: $E_{11} = 144$ GPa, $E_{22} = E_{33} = 9.68$ GPa, $G_{12} = G_{13} = 4.14$ GPa, $G_{23} = 3.45$ GPa, $\nu_{12} = \nu_{13} = 0.3$, $\nu_{23} = 0.5$, and the density $\rho = 1389$ kg/m^3. Although the damping coefficients could be the subject of uncertainty, in this study they are assumed to be $\xi_1 = 0.05$ and $\xi_2 = 0.05$ just for computational purposes. Four random variables are selected for the orientation angles of the fibre reinforcement according to the common stacking sequences employed in the construction of composite structures. These random variables have the following expected values: $\mathcal{E}\{V_1\} = 0°$, $\mathcal{E}\{V_2\} = 15°$, $\mathcal{E}\{V_3\} = 45°$ and $\mathcal{E}\{V_4\} = 90°$. On the other hand the expected values of random variables V_i, $i = 5, \ldots, 10$ correspond to the nominal values of the elastic properties indicated above.

The stacking sequences to be used in this study are the ones described in Table 2. The acronyms CUS and CAS mean "Circumferential Uniform Stiffness" and "Circumferential Asymmetric Stiffness". These acronyms were introduced by Rehfield et al. [7] to identify the type of lamination scheme for a rectangular cross-section. The CUS laminate involves elastic constitutive coupling between twisting moments and axial force as well as both shear forces and both bending moments, whereas the CAS laminate involves elastic constitutive coupling between bending moments and twisting moments together with coupling of the axial force with both shear forces [12,29,7]. Although "I" and rectangular cross-sections

Table 2
Lamination schemes for the cross-sections.

Cross-section	Laminate name	Angle orientation
I	Quasi Isotropic	web: $\{0°,-45°,45°,90°\}_S$ flanges: $\{0°,-45°,45°,90°\}_S$
	Angle-ply	web: $\{(\alpha,-\alpha)_2\}_S$ flanges: $\{(\alpha,-\alpha)_2\}_S$
	CUS (α)	web: $\{(0°,90°)_2\}_S$ flanges: $\{(0°,90°)_3,\alpha,\alpha\}$
□	CUS (α)	left and right panels: $\{(\alpha,\alpha)_4\}$ upper and lower panels: $\{(\alpha,\alpha)_4\}$
	CAS (α)	upper and right panels: $\{(\alpha,\alpha)_4\}$ lower and left panels: $\{(-\alpha,-\alpha)_4\}$

have evidently different shapes, they can manifest a similar elastic behavior depending on the type of laminates employed in their construction. That is, in the case of an "I" cross-section the terms "CUS" or "CAS" are associated with the similar elastic constitutive coupling observed in "CUS" or "CAS" stacking sequences of the rectangular cross-section. It should be taken into account that the quasi-isotropic and angle-ply laminates produce a slight constitutive elastic coupling between normal and shear components of strains and stresses of the shell, which can eventually couple internal bending moments and twisting moments [29].

Models of twelve finite elements of five nodes are used for the deterministic and stochastic calculations. This number of elements was shown [29] to be enough to guarantee a precision of more than 99% up to the eighth natural frequency. In Tables 3 and 4 it is possible to see the natural frequencies of the deterministic model with open and closed cross-sections, respectively. The nominal laminates of Table 2 were employed. Notice that the feature of the modes is also indicated in Tables 3 and 4 in the same way explained for Table 1. That is *BYY*, *BZZ* and *T* identify bending mode in *y*-direction, bending mode in *z*-direction and twisting mode, respectively; whereas *BYT* (or *BZT*), *BYZ* and *BZY* identify coupled bending-twisting modes and coupled bending-bending modes, respectively; *TYZ* and *TZY* identify twisting dominant-bending coupling, whereas *TEB* indicates a twisting-extensional-bending coupling and *TE* identify a twisting-extensional coupling. Fig. 3 shows a few examples of the coupled modes of the box-beam with CAS (45) and CUS (45). The value of the frequency is also incorporated in the figure just for clarity and comparison purposes.

The stochastic analysis is mainly concerned with the evaluation of the uncertainty propagation in the frequency response function of the composite beam subjected to a unit force F used to perturb the structure. The force is located at the free end of the beam ($x = L$) according to Fig. 2 with $\varphi = 45°$. The response is observed at the free end, and it is evaluated by means of the following frequency response function:

$$H_F(\omega) = \frac{\|\widehat{\mathbf{U}}_{\boldsymbol{P}}(\omega)\|}{\widehat{F}(\omega)}. \tag{30}$$

In Eq. (30), $\|\widehat{\mathbf{U}}_{\boldsymbol{P}}\|$ is the norm of the Fourier transform of the displacement vector of the point (calculated according to Eq. (1)), where the force is applied (see Fig. 2) and $\widehat{F}$ is the Fourier transform of the force applied at the beam's end. Moreover, other frequency response functions may be introduced for particular comparative purposes, that is:

$$H_1(\omega) = \frac{\hat{u}_{yc}(\omega)}{\widehat{F}_y(\omega)}, \quad H_2(\omega) = \frac{\widehat{u}_{zc}(\omega)}{\widehat{F}_z(\omega)}, \quad H_3(\omega) = \frac{\widehat{\phi}_x(\omega)}{\widehat{T}_x(\omega)}, \tag{31}$$

where $\hat{u}_{yc}$, $\hat{u}_{zc}$ and $\hat{\phi}_x$ are the Fourier transforms of lateral displacement, vertical displacement and twisting angle, respectively, whereas $\widehat{F}_y$, $\widehat{F}_z$ and $\widehat{T}_x$ are the Fourier transforms of the components of force F and the associated twisting moment. For this problem, the displacements are calculated at the free end.

The Fig. 4 shows an example of the convergence of the Monte Carlo simulations by studying the evolution of the function *conv* (N_{MS}) with respect to the number of simulations. In this example $\Delta_\alpha = 2°$ is employed in the laminates and the beam has an open

Table 3
Natural frequencies [Hz] of I-beams with laminates of Table 2.

Mode number	$\{0,-45,45,90\}_S$		$\{(45,-45)_2\}_S$		$\{(15,-15)_2\}_S$		CUS (15)	
	Freq	Mode	Freq	Mode	Freq	Mode	Freq	Mode
1	6.00	*BYY*	3.14	*BYY*	8.68	*BYY*	7.61	*BYZ*
2	14.11	*T*	12.43	*BZZ*	15.15	*T*	11.82	*T*
3	23.31	*BZZ*	16.08	*T*	32.37	*BZZ*	25.07	*BZY*
4	37.29	*BYY*	19.64	*BYY*	52.96	*BYT*	45.73	*BYZ*
5	55.83	*T*	52.41	*T*	69.38	*T*	58.47	*T*
6	102.95	*BYY*	54.78	*BYT*	142.29	*BYT*	102.59	*BZY*
7	129.37	*BZZ*	74.91	*BZZ*	151.94	*BZZ*	120.19	*BYZ*
8	132.49	*T*	100.13	*T*	174.04	*T*	147.63	*T*

Table 4
Natural frequencies [Hz] of box-beams with laminates of Table 2.

Mode number	CAS (15)		CAS (45)		CUS (15)		CUS (45)	
	Freq	Mode	Freq	Mode	Freq	Mode	Freq	Mode
1	13.57	*BYT*	6.07	*BYT*	12.79	*BYZ*	6.02	*BYZ*
2	24.18	*BZT*	10.52	*BZT*	23.92	*BZY*	10.49	*BZY*
3	70.09	*TYZ*	36.86	*BYT*	59.89	*TE*	36.76	*BYZ*
4	94.28	*TYZ*	62.21	*BZT*	74.14	*BYZ*	62.29	*BZY*
5	118.62	*TZY*	92.53	*TYZ*	119.46	*BZY*	75.57	*TE*
6	169.13	*TYZ*	98.75	*BYT*	180.86	*TE*	99.42	*BYZ*
7	231.64	*TZY*	120.56	*TEB*	193.94	*BYZ*	146.97	*TE*
8	266.14	*TEB*	161.77	*TYZ*	239.72	*BZY*	156.71	*BZY*

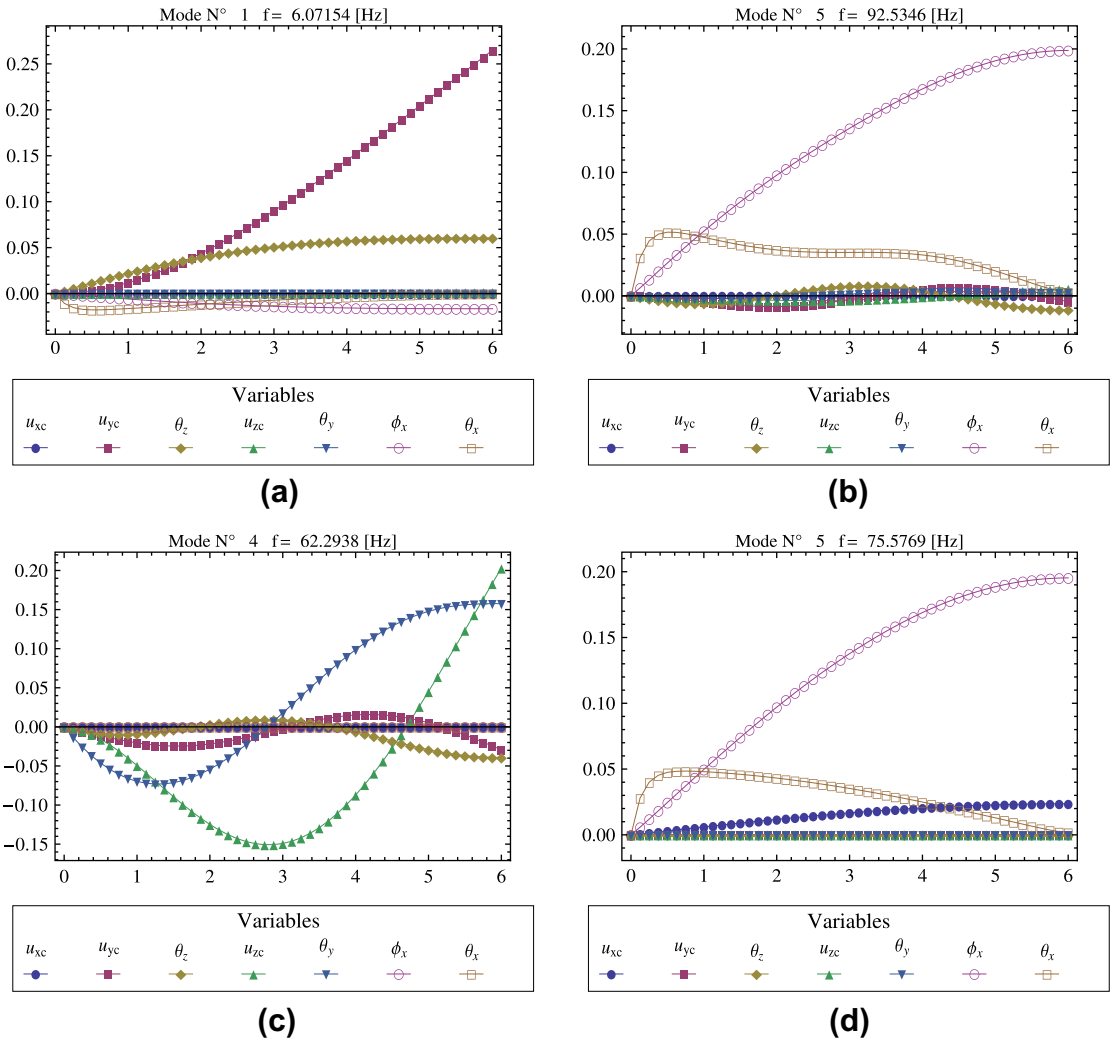

Fig. 3. Selected modes shapes of the Box-beam (from Table 4). (a) 1St mode type *BYT* for CAS (45), (b) 5th mode type *TYZ* for CAS (45), (c) 4th mode type *BZY* for CUS (45), and (d) 5th mode type *TE* for CUS (45).

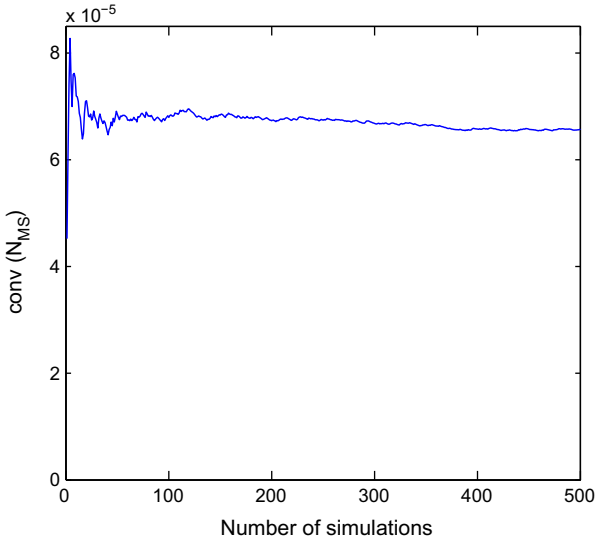

Fig. 4. Example of the convergence of a Monte Carlo simulation.

cross-section with quasi-isotropic laminates. Recall that the excitation force is unitary, i.e. $\|\boldsymbol{F}\| = 1N$ and $\varphi = 45°$. As it is possible to see in Fig. 4, a good convergence is achieved with 500 samplings, and a reasonable convergence is also achieved with 250 samplings. The simulation of all stacking sequences and cross-section in present article gave similar convergence patterns.

Figs. 5–9 illustrate the results of the simulations carried out for the stacking sequences of the open cross-section in which only the uncertainty in the laminates is considered. Fig. 5 shows the Frequency Response Functions (FRFs) of the composite beam with quasi-isotropic laminates and a dispersion parameter of $\Delta_\alpha = 2°$. In particular, Fig. 5a shows the FRF of the most relevant kinematic variables (i.e. bending displacements and the twisting parameter) of the deterministic (or mean) model according to Eq. (31), whereas Fig. 5b shows the FRF according to Eq. (30) of the mean model and the mean response of the stochastic model as well as the 95% confidence interval (CI). Now in Fig. 6 the same information is shown but for a stacking sequence of $\{(45,-45)_2\}_S$. Notice the magnitude of the uncertainty propagation in the case of the angle-ply stacking sequence in comparison to the case of a quasi-isotropic stacking sequence for the same value of the dispersion, i.e. $\Delta_\alpha = 2°$. Fig. 7 shows the same information of the previous two figures but for the laminates $\{(15,-15)_2\}_S$ and a dispersion

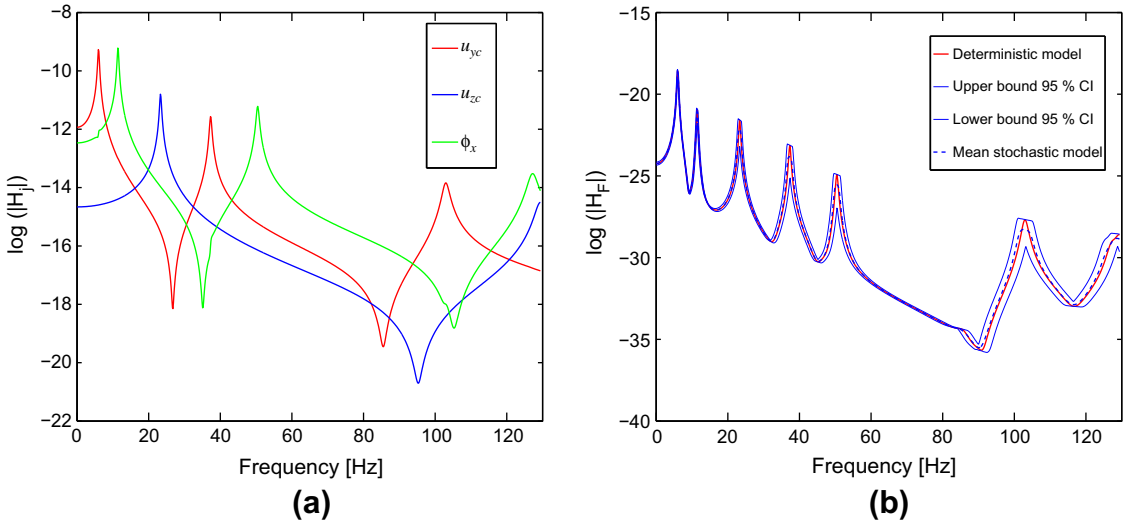

Fig. 5. FRFs of the beam with quasi-isotropic stacking sequences ($\Delta_\alpha = 2°$). (a) Kinematic variables: u_{yc}, u_{zc} and ϕ_x. (b) Displacement of the point where the load is applied.

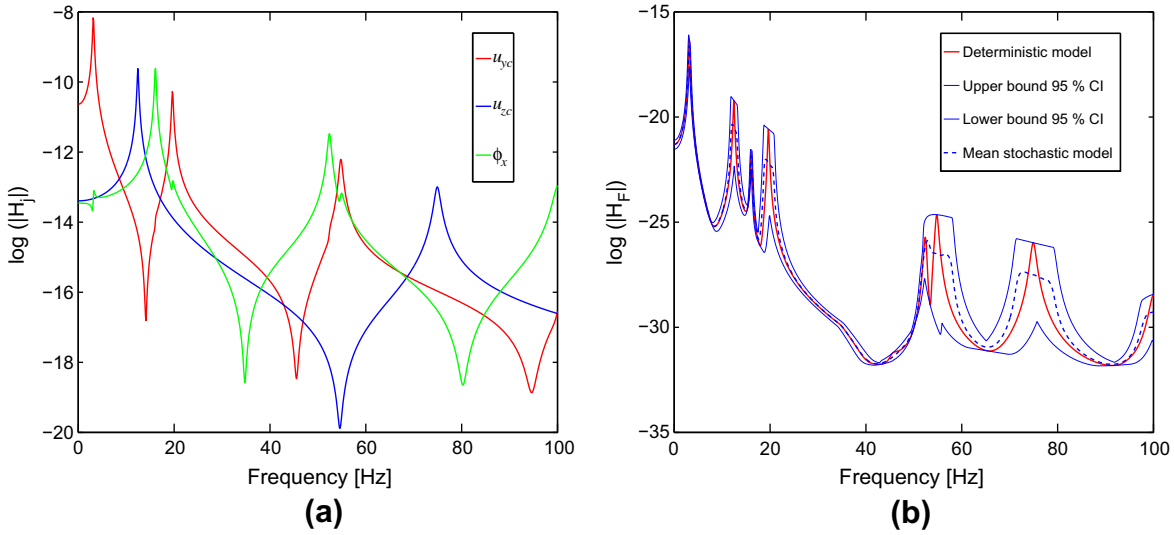

Fig. 6. FRFs of the beam with $\{(45, -45)_2\}_S$ stacking sequences ($\Delta_\alpha = 2°$). (a) Kinematic variables: u_{yc}, u_{zc} and ϕ_x. (b) Displacement of the point where the load is applied.

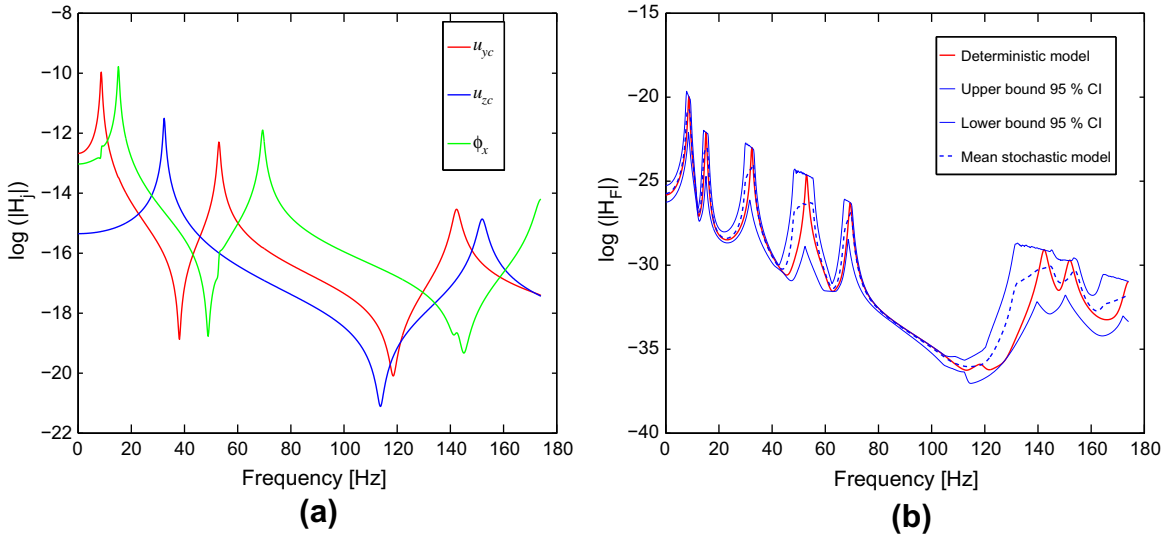

Fig. 7. FRFs of the beam with $\{(15, -15)_2\}_S$ stacking sequences ($\Delta_\alpha = 5°$). (a) Kinematic variables: u_{yc}, u_{zc} and ϕ_x. (b) Displacement of the point, where the load is applied.

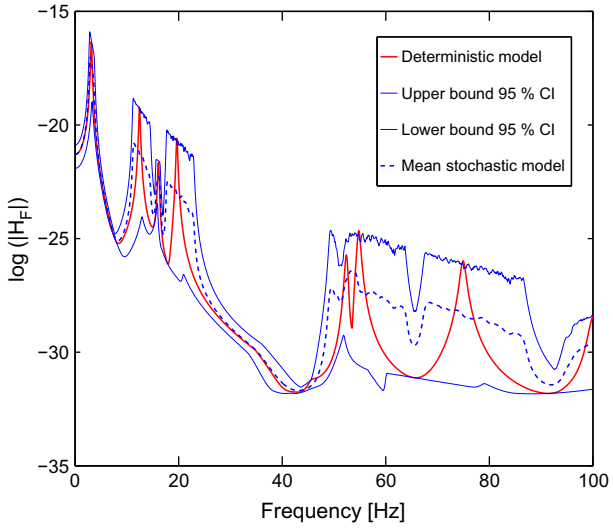

Fig. 8. FRF of the beam with $\{(45, -45)_2\}_S$ stacking sequences and $\Delta_\alpha = 5°$.

parameter $\Delta_\alpha = 5°$. In this type of lamination appears a slight elastic coupling, observable in the FRF of u_{yc} and ϕ_x in Fig. 7a, that influences the increase of uncertainty around those modes as it is possible to see in Fig. 7b. Fig. 8 shows the FRF $H_F(\omega)$ of the beam with the angle-ply stacking sequences $\{(45, -45)_2\}_S$ for a dispersion of $\Delta_\alpha = 5°$. Comparing Figs. 8 and 6b it is possible to see that the confidence interval for $\Delta_\alpha = 5°$ is, as expected, sensibly larger than the one for $\Delta_\alpha = 2°$, except in the first lateral bending mode and the first twisting mode (actually third in the sequence), where the propagation of uncertainty is not high even if the dispersion in the laminates has been more than doubled.

As a first observation of the previous figures, it may be stated that the configuration of the laminates in the cross-section and the angular dispersion in the fiber reinforcement influence a lot the dispersion of the results. Moreover it seems that the constitutive elastic couplings have an important effect in the propagation of the uncertainty in the dynamics of thin-walled composite beams. In order to check this affirmation the following stochastic study is performed in an I-beam with a CUS stacking sequence. The fiber reinforcement has a dispersion quantified by $\Delta_\alpha = 5°$ in

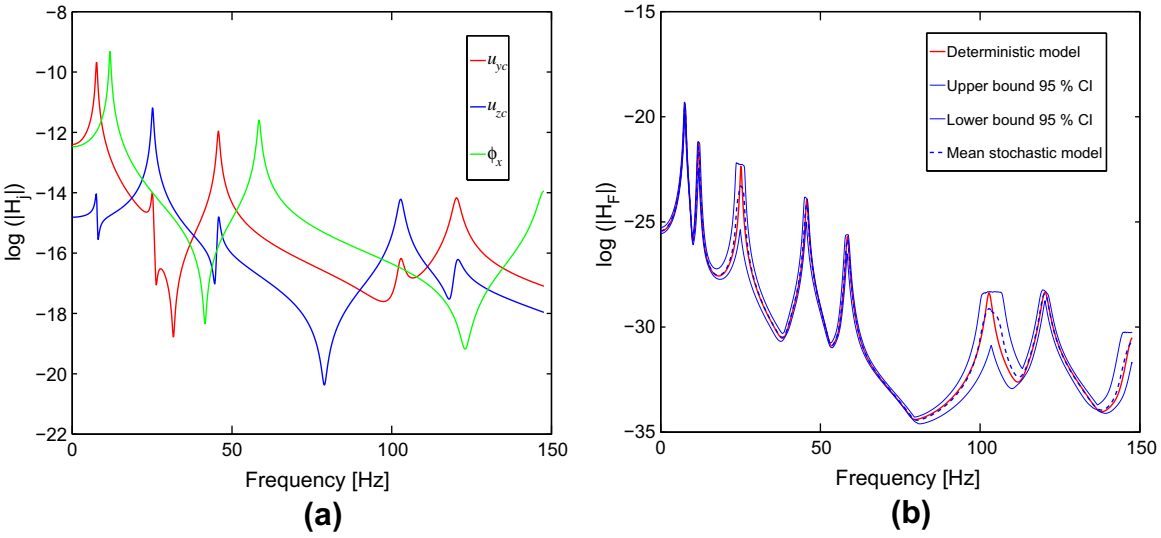

Fig. 9. FRFs of the I-beam with CUS (15) stacking sequence ($\Delta_\alpha = 5°$). (a) Kinematic variables: u_{yc}, u_{zc} and ϕ_x. (b) Displacement of the point, where the load is applied.

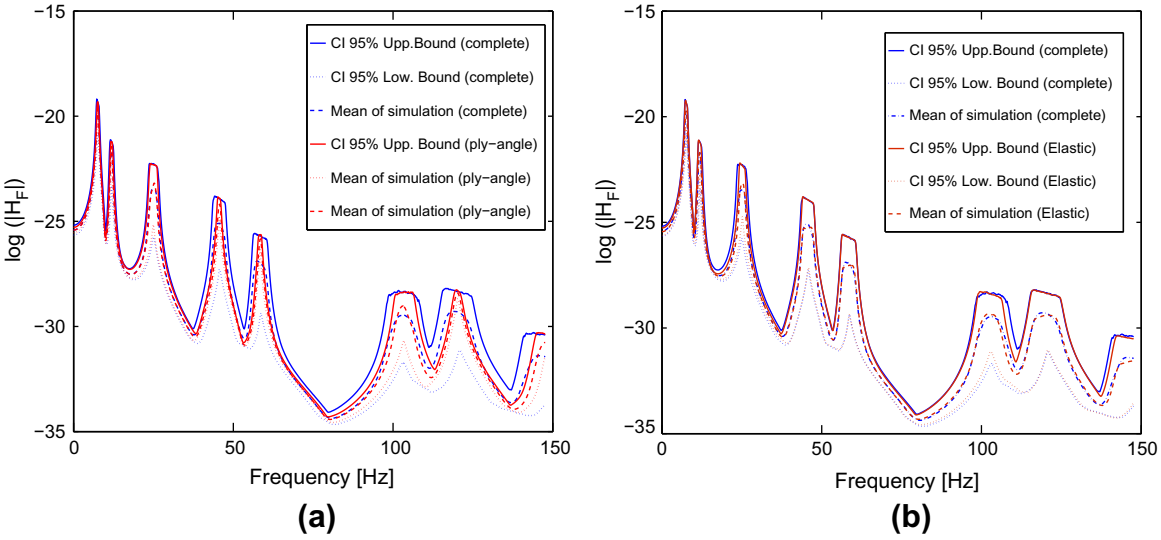

Fig. 10. Comparisons of FRFs for I-beam with CUS (15) laminate. (a) Ply-angle vs complete uncertainties and (b) elastic vs complete uncertainty.

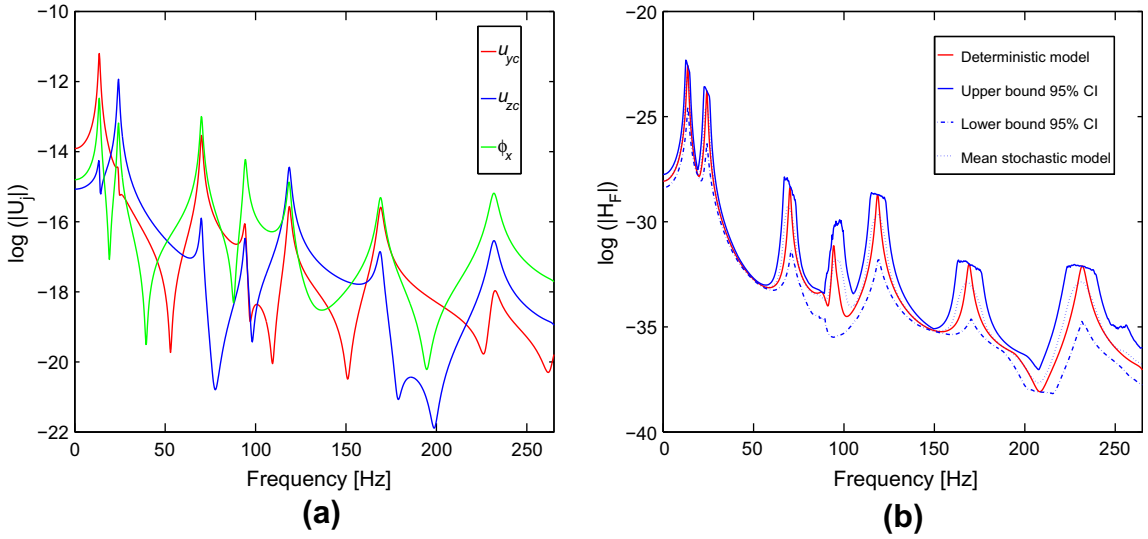

Fig. 11. FRFs of the box-beam with CAS (15) ($\Delta_\alpha = 2^\circ, \delta_{V_i} = 0.05$). (a) Kinematic variables: u_{yc}, u_{zc} and ϕ_x. (b) Displacement of the point where the load is applied (with complete uncertainty).

the configuration CUS (15). Fig. 9 shows the dynamic responses of the I-beam with CUS configuration. In fact, Fig. 9a depicts the FRF of the kinematic variables u_{yc}, u_{zc} and ϕ_x measured at the free end, whereas Fig. 9b shows the FRF according to Eq. (30) of the mean model and the mean response of the stochastic model as well as the 95% confidence interval. It is noticeable from Fig. 9a that modes 1, 3, 4, 6 and 7 have a bending-bending coupled character. On the other hand modes 2 and 5 have a twisting character. Recall that the dispersion in the fiber orientation is quantified by $\Delta_\alpha = 5^\circ$, which in other stacking sequences, produce a huge effect of uncertainty propagation. However in the case of a CUS lamination (with $\alpha = 15^\circ$) it appears that the uncertainty propagation have more influence in the coupled *BZY* modes (such as the sixth and third modes) than in the coupled *BYZ* modes (such as the first, fourth and seventh mode) as one can check in the Fig. 9b.

As shown in the previous figures, the uncertainty related exclusively to the geometric parameters (reinforcement angle of the fibers) can propagate more or less depending on the frequency order and certain lamination schemes. In fact, the uncertainty in the frequency response functions of structural systems propagates more extensively in the higher modes. An aspect that was already observed in others studies with isotropic Timoshenko beams [36]. Nevertheless, the dynamic response can be altered not only by uncertainty in geometric (or constructive) aspects but also due to the uncertainty in the elastic properties.

As mentioned above, in the construction of the stochastic model, the random variables featuring the elastic properties have bounds defined by a coefficient of variation $\delta_{V_i} \in [0.04, 0.12]$, $i = N_P + 1, \ldots, N_P + 6$. Despite the wide variability observed in some elastic properties (e.g. Poisson coefficients $\delta_{\nu_{12}} = 0.12$ [19]), in this paper a coefficient of variation common to all random variables representing the elastic properties is employed. Specifically, the coefficient of variation has to be relatively low (e.g. $\delta_{V_i} = 0.05$) in order to evaluate its global influence on the propagation of uncertainty related to elastic properties.

Now, Fig. 10 shows the FRFs of the I-beam, with laminate CUS (15), in the point where the load is applied. The random variables are defined such that $\Delta_\alpha = 5^\circ$ and $\delta_{V_i} = 0.05$. Three circumstances are shown in these pictures: the case in which all parameters are uncertain (complete uncertainty), the case in which only the ply-angle parameters are uncertain (ply-angle uncertainty) and the case in which only material elastic parameters (elastic

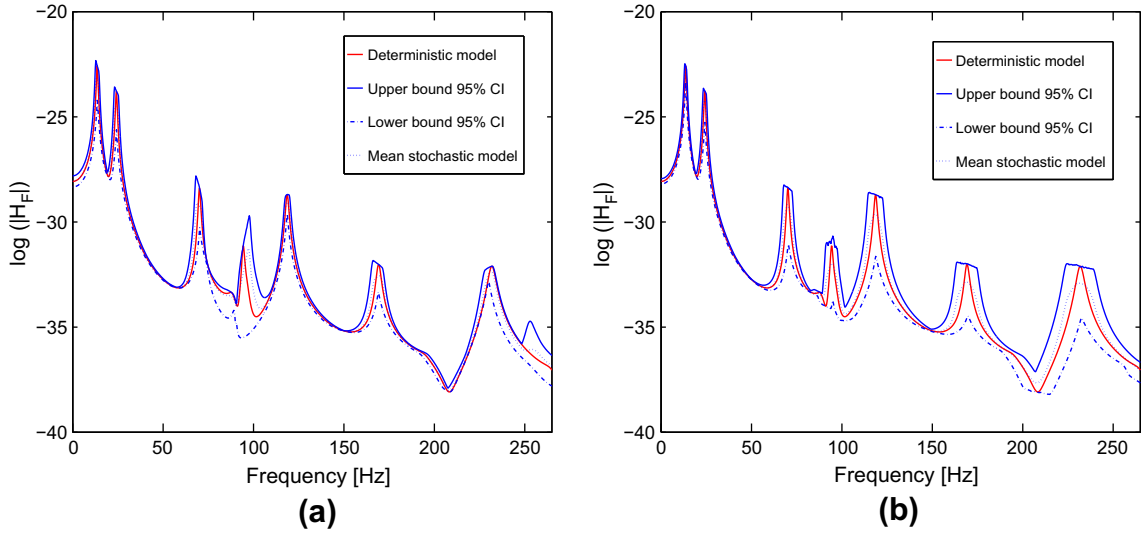

Fig. 12. Comparisons of the box-beam with CAS (15) ($\Delta_\alpha = 2^\circ, \delta_{V_i} = 0.05$). (a) Only ply-angle uncertainties and (b) only elastic uncertainty.

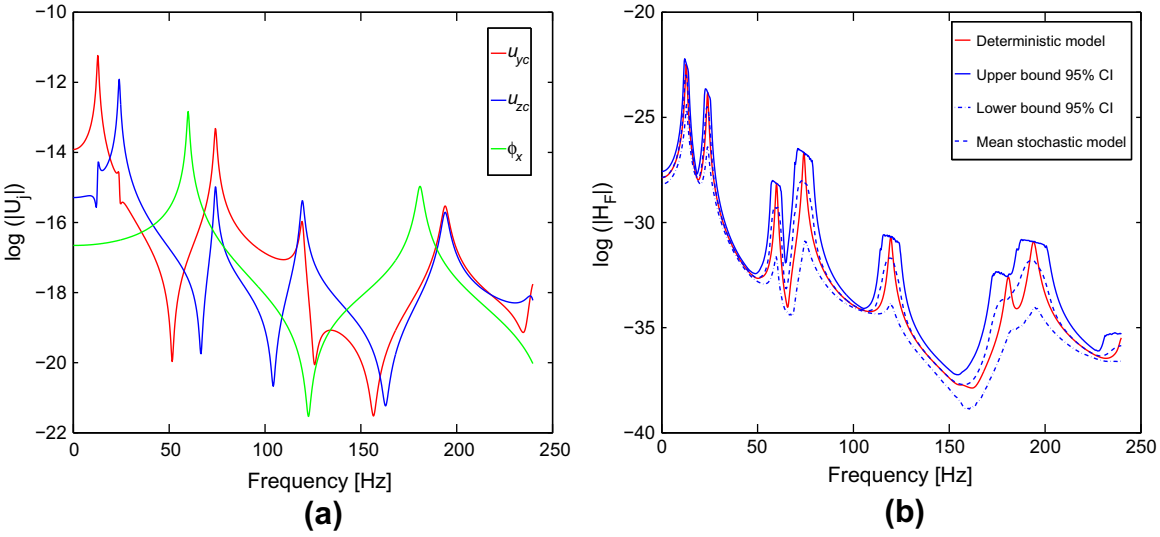

Fig. 13. FRFs of the box-beam with CUS (15) ($\Delta_\alpha = 2°$, $\delta_{V_i} = 0.05$). (a) Kinematic variables: u_{yc}, u_{zc} and ϕ_x. (b) Displacement of the point, where the load is applied (with complete uncertainty).

uncertainty). Fig. 10a compares the 95% confidence intervals of the responses if the complete and ply-angle uncertainty, whereas Fig. 10b compares the 95% confidence intervals of the responses if the complete and elastic uncertainty. It is remarkable for this type of cross-section and lamination that a relatively small coefficient of variation in the elastic properties has more influence than a relatively important dispersion of the fiber orientation angles.

Figs. 11 and 12 illustrate the FRFs of the box beam with a CAS (15) configuration. The simulations were carried out for $\Delta_\alpha = 2°$ and $\delta_{V_i} = 0.05$, $i = 5, \ldots, 10$ in the appropriate random variables, that correspond to possible variability in the construction of composite structures [19]. Fig. 11a illustrates the deterministic FRFs of the most representative bending and twisting kinematic variables of the beam model. It is possible to see the highly coupled character of the beam dynamics which is associated to the constitutive elastic coupling of the CAS (15) stacking sequence. It is interesting to check the FRFs pattern of Fig. 11a with the corresponding values and modes indicated in Table 4. Fig. 11b compares the deterministic response and the mean response of the stochastic model as well as the 95% confidence interval of the random response. For this figure both sets of parameters were considered uncertain with their corresponding uncertainty measure (Δ_α or δ_{V_i}). Fig. 12a shows the FRFs of the deterministic and stochastic models considering only the ply-angle uncertainty, on the other hand Fig. 12b shows the same responses but considering only uncertainty in the elastic properties. Although in some cases the ply-angle uncertainty can affect substantially the response (e.g. fourth mode in Fig. 12a); the typical uncertainty associated to elastic properties has generally more influence than the one related to ply-angles, as it is possible to see in the precedent figures. Figs. 13 and 14 show the same information of the previous two figures but for the lamination case CUS (15) in a box-beam. The frequency response functions of the beam with CUS (15) laminates have a similar behavior to the one observed in the beam with the CAS (15) stacking sequence, although the influence of the ply-angle uncertainty is a little-bit.

The responses of the box-beam with CAS (45) laminates can be observed in Figs. 15 and 16. Although CAS (15) and CAS (45) have in essence the same type of elastic coupling, both differ in the elastic coupling intensity. Nevertheless, the ply-angle uncertainty appear to be as important as the elastic uncertainty in the stochastic response of CAS (45) laminates as can be observed in Fig. 16a and b.

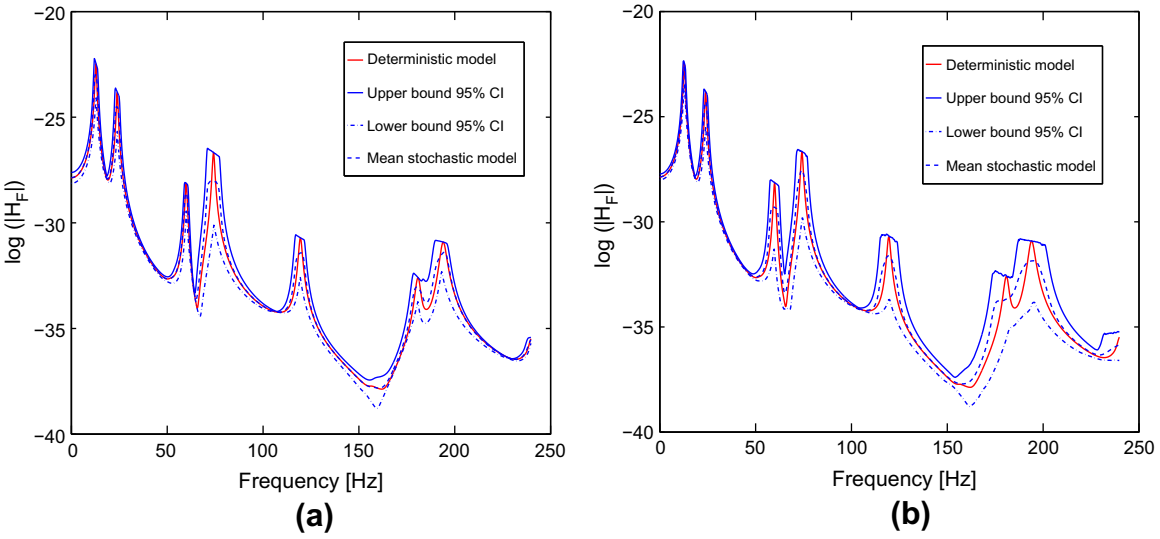

Fig. 14. Comparisons of the box-beam with CUS (15) ($\Delta_\alpha = 2°$, $\delta_{V_i} = 0.05$). (a) Only ply-angle uncertainties and (b) only elastic uncertainty.

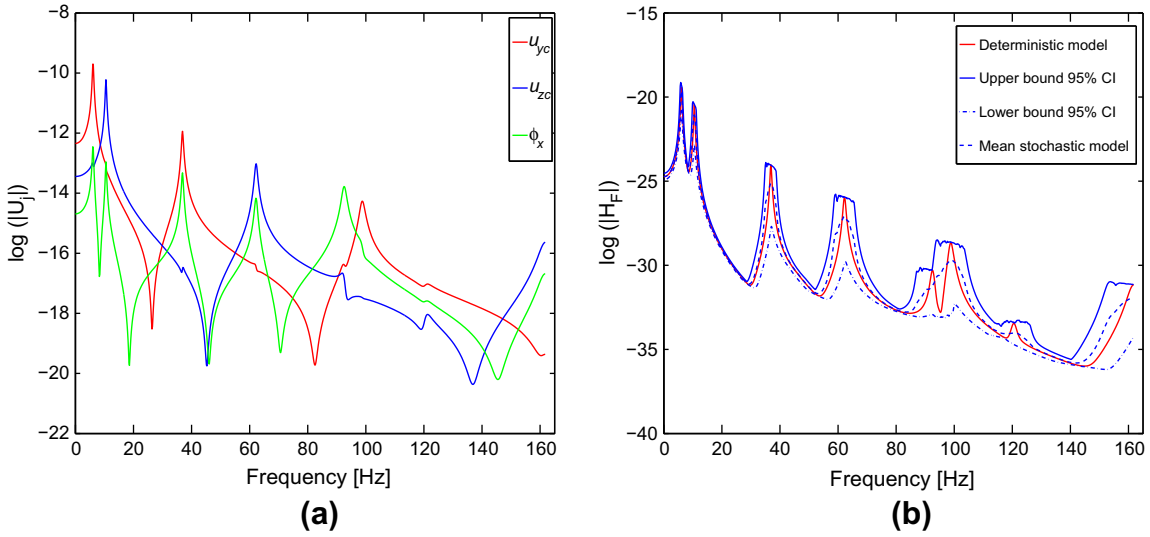

Fig. 15. FRFs of the box-beam with CAS (45) ($\Delta_\alpha = 2°$, $\delta_{V_i} = 0.05$). (a) Kinematic variables: u_{yc}, u_{zc} and ϕ_x. (b) Displacement of the point where the load is applied (with complete uncertainty).

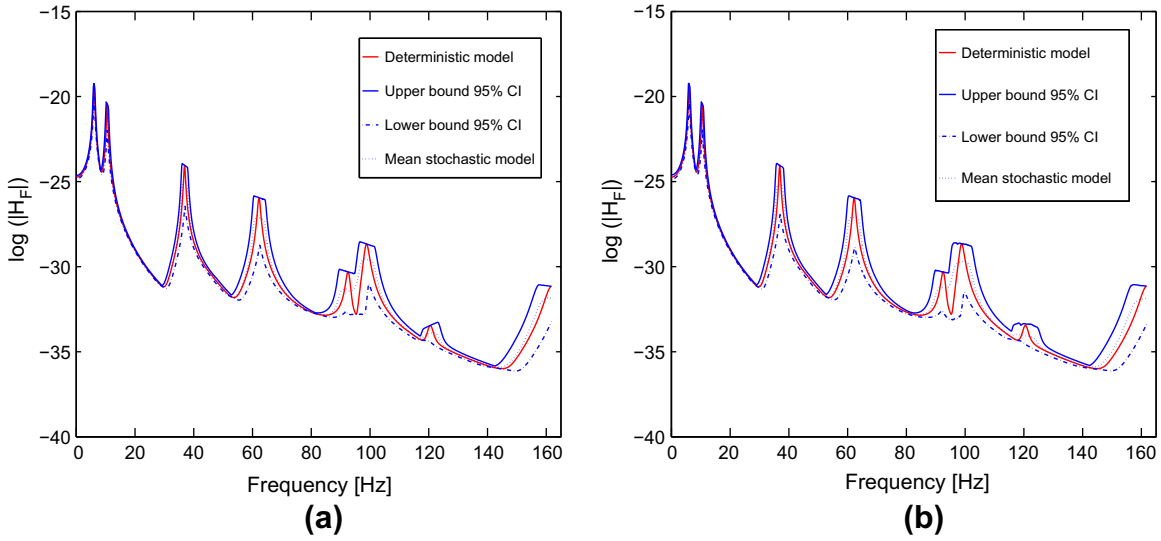

Fig. 16. Comparisons of the box-beam with CAS (45) ($\Delta_\alpha = 2°$, $\delta_{V_i} = 0.05$). (a) Only ply-angle uncertainties and (b) only elastic uncertainty.

5. Conclusions

In this article a study about the influence of uncertainty in the dynamics of thin-walled fiber reinforced composite beams has been carried out. In this study a thin-walled beam model for composite materials has been employed as the deterministic model, whose numerical outcome represents the expected response. Thereafter the stochastic model has been constructed by introducing random variables associated to the uncertain parameters of the problem. The parameters selected for the studies of uncertainty propagation were the elastic properties of the composite material and the orientation angles of fiber reinforcement in the laminates. The probability density functions of each random variable have been derived according to the Maximum Entropy Principle. Typical open and closed cross-section with several types of stacking sequences have been evaluated. From the calculation carried out in this article, the following items can be concluded:

- The propagation of uncertainty is strongly influenced by the panel laminates of the cross-section and the type of elastic coupling inherent to them.
- The propagation of uncertainty is larger in the cases where strong constitutive couplings are present (e.g. CAS laminates in rectangular cross-sections).
- Angle-ply laminates are quite sensitive to the uncertainty of the fiber orientation.
- Stacking sequences with an important number of plies oriented in the main orthotropic directions (i.e. $\alpha = 0°$ or $\alpha = 90°$) proved to be robust with respect to the variability of the ply angle, especially in the case of non-coupled modes.
- If the beam is mainly constructed with laminates that have an important number of plies oriented in the main orthotropic directions, the principal source of uncertainty propagation is due to the uncertainty of the material elastic properties.

- If the beam is constructed with laminates that lead to strong elastic coupling, the main source of uncertainty propagation is related to the uncertainty of the fiber reinforcement angle.
- For laminates oriented in $\alpha = 45°$ (CAS, CUS or angle-ply), the uncertainty of angle-ply orientation is more influent than the uncertainty associated to the material elastic properties.

Composite structures have notable features of uncertainty as observed in the previous sections. The parametric probabilistic approach employed in this work has been a useful tool to quantify the uncertainty and to explore its propagation in the linear dynamics of the thin-walled composite beams. However, there are other concerns associated with the uncertainty of the model itself that cannot be analyzed even with a meticulous selection of uncertain parameters and associated random variables (and consequently their probability density functions), for example, the uncertainty in structural damping or the formulation of shear deformations or warping effects and their influences in the dynamics of beams or the variation of properties along the beam length. This type of problems can be faced with other tools such as Monte Carlo Markov Chain approaches or the non-parametric probabilistic approach. Also elastic properties may be correlated random variables and their influence should be analyzed. However these matters would be part of further extensions to the present contribution.

Acknowledgements

The support of Universidad Tecnológica Nacional and CONICET of Argentina and FAPERJ and CNPq of Brazil is recognized.

Appendix A. Extended definition of matrices and vectors present in the principle of virtual works

The vector of external forces $\widetilde{\mathbf{P}}_X$ and the matrix of mass coefficients $\mathbf{M}_m$ can be calculated in the following form:

$$\widetilde{\mathbf{P}}_X = \int_A \begin{bmatrix} \overline{X}_x & \overline{X}_y & \overline{X}_z \end{bmatrix} \mathbf{G}_m \, dy \, dz, \tag{A.1}$$

$$\mathbf{M}_m = \int_A \rho(y,z) \mathbf{G}_m^T \mathbf{G}_m \, dy \, dz, \tag{A.2}$$

where $\overline{X}_x$, $\overline{X}_y$ and $\overline{X}_z$ are general volume forces, whereas:

$$\mathbf{G}_m = \begin{bmatrix} 1 & 0 & -y & 0 & z & 0 & -\omega \\ 0 & 1 & 0 & 0 & 0 & -z & 0 \\ 0 & 0 & 0 & 1 & 0 & y & 0 \end{bmatrix}, \tag{A.3}$$

The vector of natural boundary conditions $\widetilde{\mathbf{B}}_X$ can be written in the subsequent form:

$$\widetilde{\mathbf{B}}_X = \begin{Bmatrix} -\overline{Q}_x + Q_x \\ -\overline{Q}_y + Q_y \\ -\overline{M}_z + M_z \\ -\overline{Q}_z + Q_z \\ -\overline{M}_y + M_y \\ -\overline{T}_{sv} - \overline{T}_w + T_{sv} + T_w \\ -\overline{B} + B \end{Bmatrix}, \tag{A.4}$$

where $\overline{Q}_x$, $\overline{Q}_y$, $\overline{Q}_z$, $\overline{M}_y$, $\overline{M}_z$, $\overline{T}_w$ and $\overline{T}_{sv}$ are prescribed forces applied at the boundaries.

References

[1] Barbero E. Introduction to composite material design. NY (USA): Taylor and Francis Inc.; 1999.
[2] Jones R. Mechanics of composite material. NY (USA): Taylor and Francis Inc.; 1999.
[3] Daniel IM, Ishai O. Engineering mechanics of composite materials. 2nd ed. NY (USA): Oxford University Press Inc.; 2006.
[4] Bauld N, Tzeng L. A Vlasov theory for fiber-reinforced beams with thin-walled open cross sections. Int J Solids Struct 1984;20(3):277–97.
[5] Kapania R, Raciti S. Recent advances in analysis of laminated beams and plates. 1. Shear effects and buckling. AIAA J 1989;27(7):923–34.
[6] Bauchau O. A beam theory for anisotropic materials. J Appl Mech 1985;52(2):416–22.
[7] Rehfield L, Atilgan A, Hodges D. Non-classical behavior of thin-walled composite beams with closed cross sections. J Am Helicopter Soc 1990;35(3):42–50.
[8] Librescu L, Song O. On the aeroelastic tailoring of composite aircraft swept wings modeled as thin-walled beam structures. Compos Eng 1992;2(5–7):497–512.
[9] Song O, Librescu L. Free vibration of anisotropic composite thin-walled beams of closed cross-section contour. J Sound Vib 1993;167(1):129–47.
[10] Cesnik C, Sutyrin V, Hodges D. Refined theory of composite beams: the role of short-wavelength extrapolation. Int J Solids Struct 1996;33(10):1387–408.
[11] Cortínez VH, Piovan Mt. Vibration and buckling of composite thin-walled beams with shear deformability. J Sound Vib 2002;258(4):701–23.
[12] Piovan MT, Cortínez VH. Mechanics of shear deformable thin-walled beams made of composite materials. Thin-Walled Struct 2007;45:37–62.
[13] Piovan MT, Cortínez VH. Mechanics of thin-walled curved beams made of composite materials, allowing for shear deformability. Thin-Walled Struct 2007;45:759–89.
[14] Carrera E, Giunta G, Petrolo M. Beam structures: classical and advanced theories. Wiley; 2011.
[15] Giunta G, Biscani F, Belouettar S, Carrera E. Analysis of thin-walled beams via a one-dimensional unified formulation through a Navier-type solution. Int J Appl Mech 2011;3:407–34.
[16] Carrera E, Varello A. Dynamic response of thin-walled structures by variable kinematic one-dimensional models. J Sound Vib 2012;331(24):5268–82.
[17] Catapano A, Giunta G, Belouettar S, Carrera E. Static analysis of laminated beams via a unified formulation. Compos Struct 2011;94(1):75–83.
[18] Giunta G, Biscani F, Belouettar S, Ferreira AJM, Carrera E. Free vibration analysis of composite beams via refined theories. Compos Part B: Eng 2013;44(1):540–52.
[19] Sriramula S, Chryssantopoulos M. Quantification of uncertainty modelling in stochastic analysis of FRP composites. Compos: Part A 2009;40:1673–84.
[20] Pawar P. On the behavior of thin-walled composite beams with stochastic properties under matrix cracking damage. Thin-Walled Struct 2011;49:1123–31.
[21] Giunta G, Carrera E, Belouettar S. Free vibration analysis of composite plates via refined theories accounting for uncertainties. Shock Vib 2011;18(4):537–54.
[22] Lutes L, Sarkani S. Stochastic analysis of structural and mechanical vibrations. New Jersey (USA): Prentice-Hall; 1997.
[23] Onkar A, Yadav D. Forced nonlinear vibration of laminated composite plates with random material properties. Compos Struct 2005;70:334–42.
[24] Mehrez L, Doostan A, Moens D, Vandepitte D. Stochastic identification of composite material properties from limited experimental databases, Part II: Uncertainty modelling. Mech Syst Signal Process 2012;27:484–98.
[25] Mehrez L, Moens D, Vandepitte D. Stochastic identification of composite material properties from limited experimental databases, Part I: Experimental database construction. Mech Syst Signal Process 2012;27:471–83.
[26] Ritto TG, Sampaio R. Stochastic drill-string dynamics with uncertainty on the imposed speed and on the bit-rock parameters. Int J Uncertainty Quantification 2011;2(2):111–24.
[27] Jaynes E. Probability theory: the logic of science, vol. 1. Cambridge (UK): Cambridge University Press; 2003.
[28] Shannon CE. A mathematical theory of communication. Bell Syst Tech 1948;27:379–423 (623–659).
[29] Piovan MT. Theoretical and computational study on the mechanics of thin-walled curved composite beams considereing non-conventional effects. PhD Thesis. Departamento de Ingeniería, Universidad Nacional del Sur, 2003 [in Spanish:Estudio Teórico y computacional sobre la mecánica de vigas curvas de materiales compuestos con secciones de paredes delgadas considerando efectos no convencionales].
[30] Na S, Librescu L. Dynamic response of elastically tailored adaptive cantilevers of nonuniform cross section exposed to blast pressure pulses. Int J Impact Eng 2001;25(9):847–67.
[31] Bathe KJ. Finite element procedures in engineering analysis. Englewood Cliffs (New Jersey, USA): Prentice-Hall; 1996.
[32] Meirovitch L. Principles and techniques of vibrations. Upper Saddle River (New Jersey, USA): Prentice-Hall; 1997.
[33] Gayathri P, Umesh K, Ganguli R. Effect of matrix cracking and material uncertainty on composite plates. Reliab Eng Syst Saf 2010;95:716–28.
[34] Vinckenroy GV, de Wilde WP. The use of Monte Carlo techniques in statistical finite element methods for the determination of the structural behaviour of composite materials structural components. Compos Struct 1995;32(1–4):247–53.
[35] Nader JW, Dagher HJ, Lopez-Anido R, Chiti FE, Fayad GN, Thomson L. Probabilistic finite element analysis of modified ASTM D3039 tension test

for marine grade polymer matrix composites. J Reinf Plast Comp 2008;27(6):583–97.
[36] Ritto T, Sampaio R, Cataldo E. Timoshenko beam with uncertainty on the boundary conditions. J Brazilian Soc Mech Sci Eng 2008;30(4):295–303.
[37] Gjelsvik A. Theory of thin-walled beams. New York (USA): John Wiley and Sons Inc.; 1981.
[38] Librescu L, Thin-Walled Song O. Composite beams: theory and application. The Netherlands: Springer-Dordrecht; 2006.